PROCEEDINGS OF SCIENCE

PoS(LATTICE2024)332

Proton and neutron electromagnetic form factors using N_f=2+1+1 twisted-mass fermions with physical values of the quark masses

Constantia Alexandrou,[a,b] **Simone Bacchio,**[b] **Giannis Koutsou,**[b] **Bhavna Prasad**[b,*] **and Gregoris Spanoudes**[a]

[a] *Department of Physics, University of Cyprus*

[b] *Computation-based Science and Technology Research Center, The Cyprus Institute*

We compute the electromagnetic form factors of the proton and neutron using lattice QCD with $N_f = 2 + 1 + 1$ twisted mass clover-improved fermions and quark masses tuned to their physical values. Three ensembles with lattice spacings of a=0.080 fm, 0.068 fm, and 0.057 fm, and approximately the same physical volume allow us to obtain the continuum limit directly at the physical pion mass. Several values of the source-sink time separation ranging from 0.5 fm to 1.5 fm are used, enabling a thorough analysis of excited state effects via multi-state fits. The disconnected contributions are analyzed using high statistics for the two-point functions combined with low-mode deflation and hierarchical probing for the fermion loop estimation. We study the momentum dependence of the form factors using the z-expansion and dipole Ansaetze, thereby enabling the extraction of the electric and magnetic radii, as well as the magnetic moments in the continuum limit, for which we provide preliminary results.

The 41st International Symposium on Lattice Field Theory (LATTICE2024)
28 July - 3 August 2024
Liverpool, UK

*Speaker

© Copyright owned by the author(s) under the terms of the Creative Commons Attribution-NonCommercial-NoDerivatives 4.0 International License (CC BY-NC-ND 4.0).

1. Introduction

The proton and neutron electromagnetic form factors offer insights into the rich internal electromagnetic structure of these nucleons. Over the years, several experimental probes have investigated these form factors, leading to a very precise determination of the charges, moments, and radii of these nucleons [1–5]. In these proceedings, we provide a calculation of the electromagnetic form factors of the nucleon using lattice QCD on three ensembles of clover-improved twisted mass fermions with two degenerate light, strange, and charm quarks ($N_f = 2 + 1 + 1$) with masses tuned to their physical values (physical point). The lattice spacings span a=0.080 fm, 0.068 fm, and 0.057 fm, allowing a continuum limit directly at the physical pion mass, while source-sink time separation ranging from 0.5 fm to 1.5 fm are used for analysis of excited states. Including disconnected contributions, we obtain the proton and neutron electric and magnetic form factors in the isospin limit and study their momentum dependence to extract the electric and magnetic radii, as well as the magnetic moments in the continuum limit.

2. Nucleon Electromagnetic form factors

In the flavor isospin limit, the electromagnetic form factors are given in terms of the matrix element of the electromagnetic current between nucleon states,

$$\langle N(p',s')|O^V_\mu|N(p,s)\rangle = \sqrt{\frac{m_N^2}{E_N(\vec{p}\,')E_N(\vec{p})}}\bar{u}_N(p',s')\Lambda_\mu(q^2)u_N(p,s)$$

with $N(p,s)$ a nucleon state of momentum p and spin s, $E_N(\vec{p}) = p_0$ its energy and m_N its mass, u_N a nucleon spinor, and $q = p' - p$ the momentum transfer from initial (p) to final (p') momentum. The matrix element is expressed in terms of the Dirac (F_1) and Pauli (F_2) form factors,

$$\Lambda_\mu(q^2) = \gamma_\mu F_1(q^2) + \frac{i\sigma_{\mu\nu}q^\nu}{2m_N}F_2(q^2), \tag{1}$$

or alternatively in terms of the nucleon electric (G_E) and magnetic (G_M) Sachs form factors via $G_E(q^2) = F_1(q^2) + \frac{q^2}{(2m_N)^2}F_2(q^2)$ and $G_M(q^2) = F_1(q^2) + F_2(q^2)$. At zero momentum transfer ($q^2 = 0$), the electric form factor yields the nucleon charge and the magnetic its magnetic moment,

$$G_E^p(0) = 1, \;\; G_E^n(0) = 0, \;\; G_M^p(0) = \mu_p, \;\; \text{and} \;\; G_M^n(0) = \mu_n, \tag{2}$$

where the superscripts p and n are used to denote the proton and neutron form factors respectively. The electric and magnetic root-mean-squared (r.m.s) radii are defined as the slope of the corresponding Sachs form factor as $q^2 \to 0$, namely

$$\langle r_X^2\rangle^{\mathsf{q}} = \frac{-6}{G_X^{\mathsf{q}}(0)}\frac{\partial G_X^{\mathsf{q}}(q^2)}{\partial q^2}\Big|_{q^2=0}, \tag{3}$$

with $X = E, M$ and $\mathsf{q} = p, n$.

PoS(LATTICE2024)332

3. Lattice setup

On the lattice, we compute the nucleon three-point correlation function,

$$C_\mu(\Gamma_\nu,\vec{q},\vec{p}\,';t_s,t_{\rm ins},t_0)=\sum_{\vec{x}_{\rm ins},\vec{x}_s} e^{i(\vec{x}_{\rm ins}-\vec{x}_0)\cdot\vec{q}}e^{-i(\vec{x}_s-\vec{x}_0)\cdot\vec{p}\,'}{\rm Tr}[\Gamma_\nu\langle\chi_N(x_s)j_\mu(x_{\rm ins})\bar{\chi}_N(x_0)\rangle], \quad (4)$$

where x_0, $x_{\rm ins}$, and x_s are referred to as the *source*, *insertion*, and *sink* respectively, and χ_N is the standard nucleon interpolating field [6]. The local vector current j_μ is given by, $j_\mu = \sum_{\mathsf{q}=u,d} e_\mathsf{q} j^\mathsf{q}_\mu = \sum_{\mathsf{q}=u,d} e_\mathsf{q}\bar{\mathsf{q}}\gamma_\mu\mathsf{q}$ where the sum over q runs over the up- ($\mathsf{q}=u$) and down- ($\mathsf{q}=d$) quark flavors and e_q is the electric charge of the quark with flavor q. We will refer to the isovector and isoscalar flavor combinations of the form factors, for which we use $j^{u-d}_\mu = j^u_\mu - j^d_\mu$ and $j^{u+d}_\mu = j^u_\mu + j^d_\mu$ respectively. The twisted mass formulation we employ allows the definition of a lattice conserved vector current which we use for the case of the connected three-point correlation functions. Γ_ν is a projector acting on dirac indices, with $\Gamma_0{=}\frac{1}{2}(1{+}\gamma_0)$ yielding the unpolarized and $\Gamma_k{=}\Gamma_0 i\gamma_5\gamma_k$ the polarized matrix elements. Without loss of generality we will take t_s and $t_{\rm ins}$ relative to the source time t_0 in what follows. The three-point function yields,

$$C_\mu(\Gamma_\nu,\vec{q},\vec{p}\,';t_s,t_{\rm ins}) = \sum_{n,m}\mathcal{A}^{n,m}_\mu(\Gamma_\nu,\vec{q},\vec{p}\,')e^{-E_n(\vec{p}\,')(t_s-t_{\rm ins})-E_m(\vec{q})t_{\rm ins}}, \quad (5)$$

where the desired ground state matrix element is $\mathcal{A}^{0,0}_\mu(\Gamma_\nu,\vec{q},\vec{p}\,')$ multiplied by unknown overlaps of the nucleon state with χ_N. To cancel these overlaps, we use the two-point nucleon correlation function,

$$C(\vec{p},t_s) = \sum_{\vec{x}_s} e^{-i\vec{x}_s\cdot\vec{p}}{\rm Tr}\left[\Gamma_0\langle\chi_N(x_s)\bar{\chi}_N(0)\rangle\right] = \sum_n c_n(\vec{p})e^{-E_n(\vec{p})t_s}, \quad (6)$$

and form the ratio,

$$\Pi^\mu(\Gamma_\nu;\vec{p}\,',\vec{q}) = \frac{\mathcal{A}^{0,0}_\mu(\Gamma_\nu,\vec{q},\vec{p}\,')}{\sqrt{c_0(\vec{p})c_0(\vec{p}\,')}}. \quad (7)$$

Ensemble	$(\frac{L}{a})^3\times(\frac{T}{a})$	a [fm]	m_π [MeV]	$m_\pi L$	$n_{\rm conf}$
`cB211.072.64`	$64^3\times128$	0.07957(13)	140.2(2)	3.62	749
`cC211.060.80`	$80^3\times160$	0.06821(13)	136.7(2)	3.78	401
`cD211.054.96`	$96^3\times192$	0.05692(12)	140.8(2)	3.90	496

Table 1: Parameters of the three $N_f = 2+1+1$ ensembles used. We provide the name of the ensemble, the lattice volume, $\beta = 6/g^2$ with g the bare coupling constant, the lattice spacing, the pion mass, the value of $m_\pi L$, and the number of configurations. The lattice spacing values and pion masses are as obtained in Ref. [7].

We use ensembles simulated with $N_f = 2+1+1$ twisted mass, clover-improved fermions with quark masses tuned to approximately their physical values. A summary of the parameters for the ensembles is provided in Table 1. The two- and three-point functions are computed using multiple source positions per gauge configuration. For two-point functions, we use 477, 650, and 480 source positions for the ensembles with decreasing a respectively. For the connected three-point functions,

PoS(LATTICE2024)332

we employ seven to ten different sink-source time separations ranging from approximately 0.5 fm to 1.5 fm with the number of source positions per configuration increasing with separation to maintain approximately constant statistical errors. We also compute the disconnected contributions to the isoscalar contribution employing the *one-end trick* [8], full dilution in color and spin, and hierarchical probing [9] to distance eight in the 4-dimensional volume for the calculation of the fermion loop. We also use eigenvector deflation for the two ensembles at coarser lattice spacings. The disconnected contributions are computed using the local vector current and therefore need to be renormalized. The renormalization is carried out non-perturbatively in the RI'-MOM scheme [10] employing momentum sources, following the procedures described in Refs. [11, 12]. We refer to Ref. [13] for details on the statistics of each sink-source separation and on the precise approach for computing the disconnected contributions.

4. Extraction of form factors

The bare form factors at each value of the momentum transfer squared (Q^2) are obtained by appropriate combinations of Γ_ν and μ depending on the momenta $\vec{p}'$ and $\vec{q}$ in $\Pi^\mu(\Gamma_\nu; \vec{p}', \vec{q})$ of Eq. (7) in order to isolate G_E and G_M. For the connected contributions we employ the standard *fixed sink* approach [6] and therefore fix $\vec{p}' = 0$. For this case, the expressions yielding G_E and G_M can be disentangled. For the disconnected contributions we combine $\vec{p}' = \frac{2\pi}{L}\vec{k}$ for $\vec{k}^2 = 0$, 1, and 2. In this case, the expressions yielding G_E and G_M cannot be disentangled (see Appendix of Ref. [6]) and we therefore use a Singular Value Decomposition to solve the overconstrained set of equations that emerge, as in the case of the Generalized Form Factors in Ref. [14].

Ensemble	$t_s^{\text{low,3pt}}$	$t_s^{\text{low,2pt}}$	$t_{\text{ins}}^{\text{max}}$
`cB211.072.64`	8, 10, 12, 14	1, 2, 3	2, 3, 4
`cC211.060.80`	8, 10, 12, 14	1, 2, 3, 4	2, 3, 4
`cD211.054.96`	8, 10, 12, 14	1, 2, 3, 4, 5	2, 3, 4

Table 2: Values of the variations used in the fit ranges for each ensemble. For each $t_{\text{ins}}^{\text{max}}$, the $t_{\text{ins}}^{\text{min}}$ takes values $t_{\text{ins}}^{\text{max}}$, $t_{\text{ins}}^{\text{max}} + 1$ or $t_{\text{ins}}^{\text{max}} + 2$.

To obtain the ground-state contribution to $\Pi^\mu(\Gamma_\nu; \vec{p}', \vec{q})$, we perform combined fits to the two- and three-point functions. We include two excited states (three-state fits) when fitting the two-point functions and the first excited state (two-state fits) when fitting the three-point function. In our fitting procedure, we first fit the two-point functions at $\vec{p}^2 = 0$ and $\vec{p}^2 = (\frac{2\pi}{L})^2$ to extract the model-averaged ground-state energy, $E_0(0)$, which is used as prior to all subsequent fits. For the ground-state energy at finite $\vec{p}$ we use the dispersion relation throughout, namely $E_0(\vec{p}) = \sqrt{E_0(0)^2 + \vec{p}^2}$. We proceed to fit each value of Q^2, allowing for different excited state energies between two- and three-point functions and between the connected isovector and isoscalar cases. In these fits, we vary the smallest separation in the two- and three-point function fits ($t_s^{\text{low,2pt}}$ and $t_s^{\text{low,3pt}}$ respectively) and the values of the insertion time included according to $t_{\text{ins}} \in [t_{\text{ins}}^{\text{min}}, t_s - t_{\text{ins}}^{\text{max}}]$. The combinations used for each ensemble are provided in Table 2.

An example of this analysis is shown in Fig. 1, where for visualization purposes we plot the ratio of three- to two-point functions of Ref. [6]. The results for each choice of fit ranges are model-

PoS(LATTICE2024)332

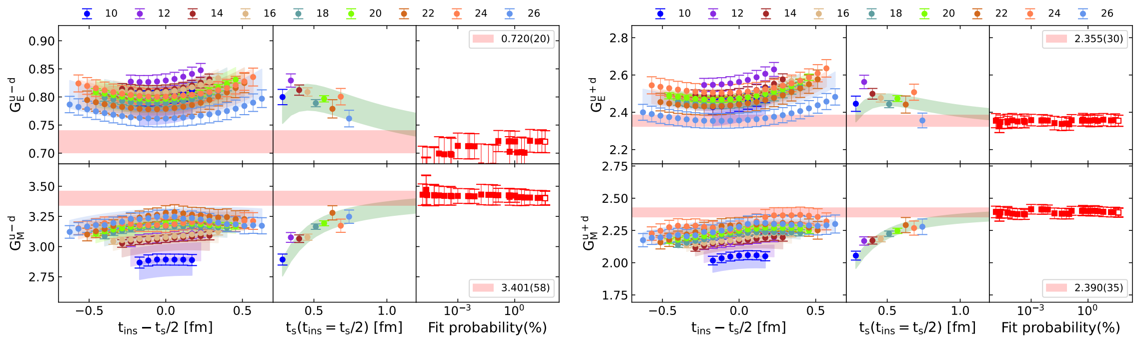

Figure 1: Extraction of the isovector (left) and isoscalar (right) electric (top) and magnetic (bottom) form factors for the second non-zero Q^2 value for the cD211.054.96 ensemble. The left column of each plot shows the ratio of three- to two-point functions described in the text for the source-sink separations indicated in the header of the figure. The center column shows the ratio for $t_{\text{ins}} = t_s/2$, and the right column gives the result of each fit versus its fit probability. The bands show the most probable fit, which is also shown with the open symbol in the right column.

averaged according to the Akaike Information Criterion (AIC) [15, 16] following the approach also employed in Ref. [17] for the axial form factors computed on the same ensembles.

5. Results for form factors

The connected and disconnected contribution to the isoscalar form factors and the isovector form factors are shown in Fig. 2 as a function of Q^2 for the three ensembles analyzed here. For each value of Q^2, the connected contributions are obtained via the analysis procedure described in the previous section. For the disconnected contributions, we do not observe significant excited state contamination within the statistical accuracy achieved and we therefore use results from plateau fits. The proton and neutron form factors are obtained from the isoscalar and isovector form factors,

$$G_X^p(q^2) = \frac{1}{2}G_X^{u-d}(q^2) + \frac{1}{6}G_X^{u+d}(q^2) \text{ and } G_X^n(q^2) = -\frac{1}{2}G_X^{u-d}(q^2) + \frac{1}{6}G_X^{u+d}(q^2), \tag{8}$$

where $X = E, M$. We model the Q^2 dependence and take the continuum limit using the proton and neutron form factors directly and fit to both dipole and z-expansion forms. The dipole is given by

$$G(Q^2) = \frac{G(0)}{1 + \frac{Q^2}{M^2}}, \tag{9}$$

with $G(0)$ and M^2 the fitting parameters. The radius is obtained via $\langle r^2 \rangle = \frac{12}{M^2}$. The z-expansion is given by

$$G(Q^2) = \sum_{k=0}^{k_{max}} a_k z^k(Q^2), \tag{10}$$

with $z = \frac{\sqrt{t_{\text{cut}}+Q^2} - \sqrt{t_{\text{cut}}}}{\sqrt{t_{\text{cut}}+Q^2} + \sqrt{t_{\text{cut}}}}$. The radius is $\langle r^2 \rangle = -\frac{3a_1}{2a_0 t_{cut}}$ and we take t_{cut}=$(2m_\pi)^2$. For the proton electric form factor we fix $G(0) = 1$ for the dipole and $a_0 = 1$ for the z-expansion. For neutron electric form factor, we use the Galster-like parameterization [18] instead of the dipole. The

PoS(LATTICE2024)332

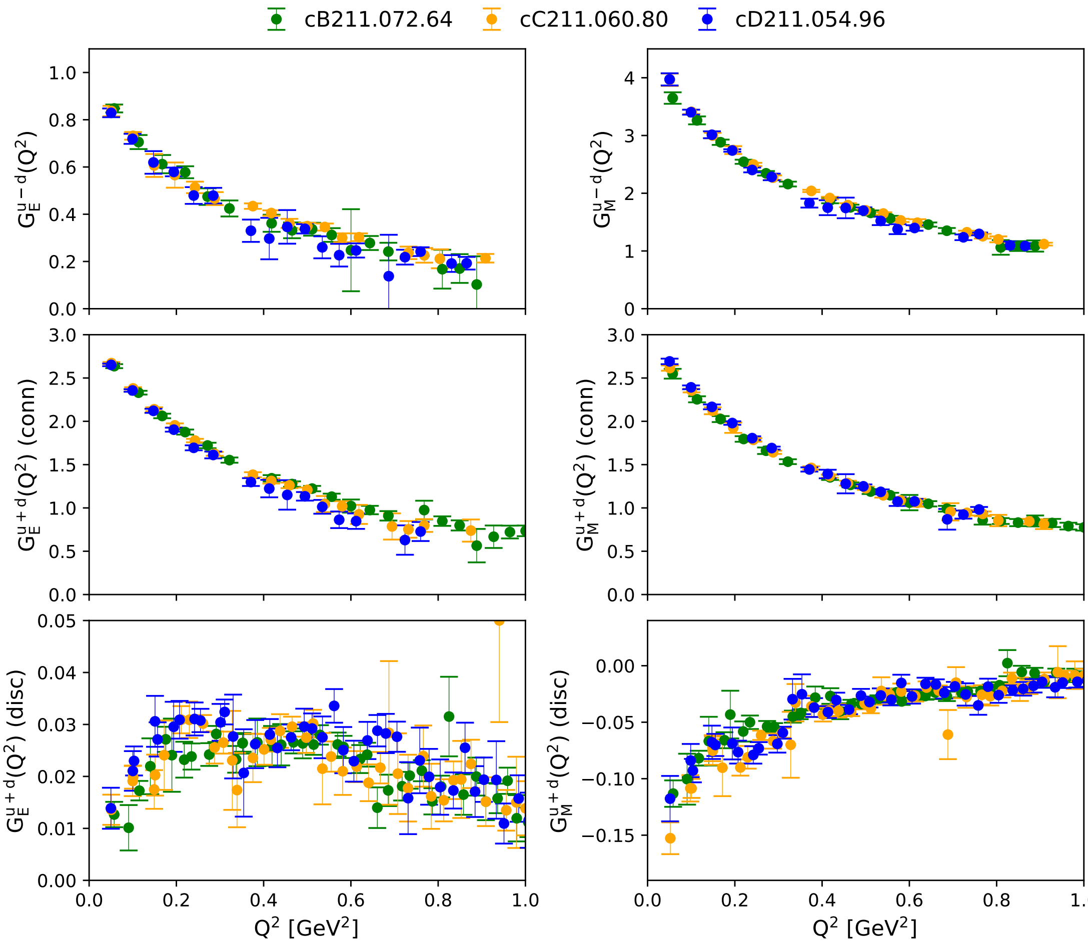

Figure 2: G_E (left) and G_M (right), connected isovector (top), connected isoscalar (center) and disconnected isoscalar (bottom) form factors as a function of Q^2 for the three ensembles analyzed here.

continuum limit is taken in two ways, namely i) via a *"two-step approach"*, where each ensemble's Q^2-dependence is fitted separately and the radius and magnetic moment are then extrapolated to the continuum in a second step or ii) via a *"one-step approach"*, where the a^2 dependence is included in the fit of either the dipole or z-expansion and all three ensembles are fitted together using a similar approach to that in Ref. [17]. We will quote results using both approaches for the dipole case while for the z-expansion we use the one-step approach. When fitting the z-expansion, we demand that the form factor approaches zero as $Q^2 \to \infty$ which fixes one parameter, and take the order of the z-expansion such that the fit has three free parameters, i.e. $k_{\max} = 4$ for the case of the electric form factors and $k_{\max} = 3$ for the magnetic.

Our results for the proton and neutron electromagnetic form factors are shown in Fig. 3, where we also show representative continuum extrapolations using either the z-expansion or dipole forms in the one-step approach. For the case of the neutron electric form factor ($G_E^n(Q^2)$) the data are consistent with the experimental values within errors. However, we do not include a^2 dependence because of large statistical errors, and restrict the maximum value of Q^2 used in the fit (Q^2_{cut}) to Q^2_{cut}

PoS(LATTICE2024)332

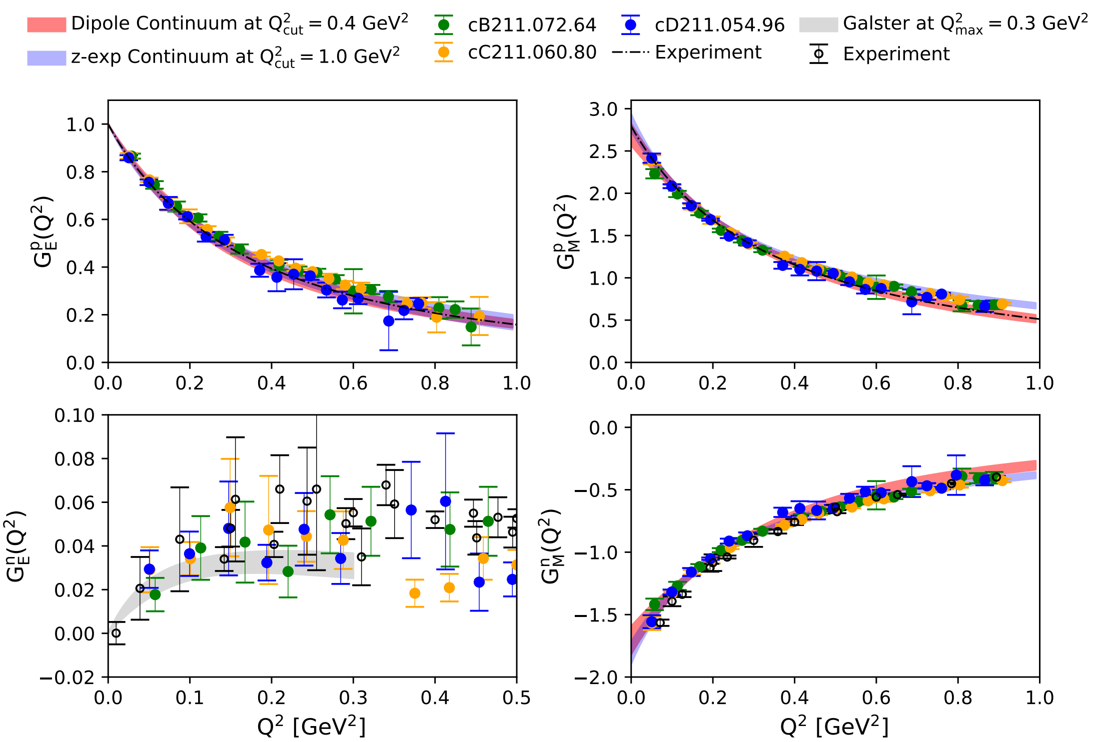

Figure 3: G_E (left) and G_M (right), proton (top) and neutron (bottom) form factors as a function of Q^2 for the three ensembles analyzed. The light red and blue bands indicate the continuum limit band using the dipole and z-expansion respectively. The black dashed lines for the proton case and the black circles for the neutron case correspond to the experimental results.

= 0.3 GeV^2 as shown in Fig. 3. For the other three form factors we vary the Q^2_{cut} in the z-expansion and use Q^2_{cut} = 0.4 GeV^2 for the dipole. In Fig. 3, we also show representatively Q^2_{cut}=0.4 GeV^2 for dipole and Q^2_{cut}=1 GeV^2 for z-expansion with $k_{\max}$ as explained in the previous section. The dashed black curves for the proton form factors are from z-expansion fits to experimental data [19]. Our results for the radii and magnetic moments are shown in Fig. 4 for all Q^2_{cut} used and for both one- or two-step approaches for the case of the dipole form. We overall observe consistent results when varying the fit ansatz and the Q^2_{cut} used. The model average result, also shown, is consistent with the PDG values [20] for these quantities.

6. Conclusions

We have carried out an analysis of the electromagnetic form factors of the nucleon using three ensembles of $N_f = 2 + 1 + 1$ twisted mass fermions at three lattice spacings and with physical pion mass. Our excited state analysis employs multi-state fits allowing for a different first excited state in the two- and three-point functions and combine multiple fit ranges via a model-average. Our results for the form factors obtained on each ensemble and the experimental results are overall compatible with each other, indicating very small cutoff effects and overall good agreement. We carry out a preliminary continuum extrapolation in a^2 within a combined fit of the Q^2-dependence

PoS(LATTICE2024)332

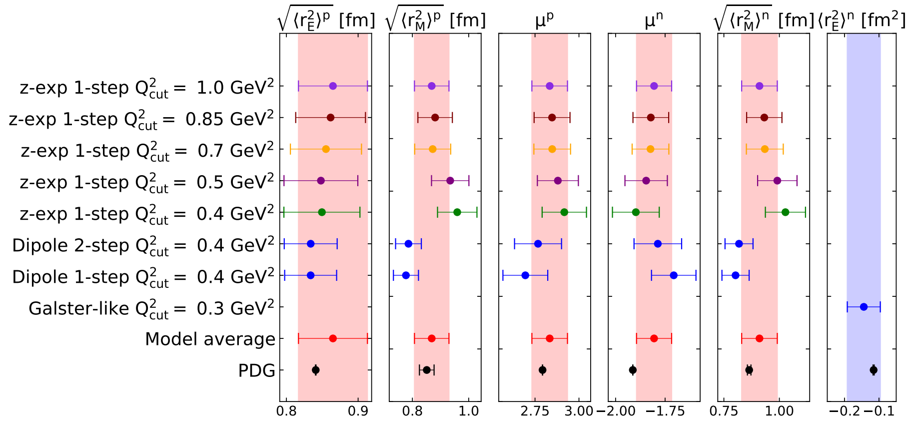

Figure 4: Electric and magnetic radii and magnetic moments of the proton and neutron for all Q^2_{cut} and, in the dipole case, using both one- or two-step approaches. The red point and band denoted "Model average" is obtained by weighting according to the AIC as explained in the text.

using both dipole and z-expansion ansaetze. Our preliminary results for the radii and magnetic moments are consistent with the PDG values for these quantities within our combined statistical and systematic errors shown in Fig. 4. The analysis of the excited state contamination, Q^2-dependence and continuum limit is continuing in order to obtain a more robust model average. We note that a fourth ensemble with lattice spacing $a = 0.049$ fm and approximately same physical volume as the three ensembles used here is available and its analysis is ongoing, with first results for the charges presented in Ref. [21].

Acknowledgments

C.A., G.K., and G.S. acknowledge partial support by the projects 3D-nucleon, NiceQuarks, and "Lattice Studies of Strongly Coupled Gauge Theories: Renormalization and Phase Transition" (EXCELLENCE/0421/0043, EXCELLENCE/0421/0195, and EXCELLENCE/0421/0025) co-financed by the European Regional Development Fund and the Republic of Cyprus through the Research and Innovation Foundation as well as AQTIVATE that received funding from the European Union's research and innovation program under the Marie Sklodowska-Curie Doctoral Networks action, Grant Agreement No 101072344. C.A acknowledges support by the University of Cyprus projects "Nucleon-GPDs" and "PDFs-LQCD". S.B. is supported by Inno4scale, which received funding from the European High-Performance Computing Joint Undertaking (JU) GA No. 101118139. B.P. is supported by ENGAGE which received funding from the EU's Horizon 2020 Research and Innovation Programme under the Marie Skłodowska-Curie GA No. 101034267. This work was supported by grants from the Swiss National Supercomputing Centre (CSCS) under projects with ids s702 and s1174. The authors gratefully acknowledge the Gauss Centre for Supercomputing e.V. (www.gauss-centre.eu) for funding this project by providing computing time through the John von Neumann Institute for Computing (NIC) on the GCS Supercomputer JUWELS-Booster at Jülich Supercomputing Centre (JSC). The authors also acknowledge the Texas Advanced Computing Center (TACC) at University of Texas at Austin for providing HPC resources.

PoS(LATTICE2024)332

References

[1] A1 collaboration, J. C. Bernauer et al., *Electric and magnetic form factors of the proton*, *Phys. Rev. C* **90** (2014) 015206 [1307.6227].

[2] V. Punjabi, C. F. Perdrisat, M. K. Jones, E. J. Brash and C. E. Carlson, *The Structure of the Nucleon: Elastic Electromagnetic Form Factors*, *Eur. Phys. J. A* **51** (2015) 79 [1503.01452].

[3] R. Pohl et al., *The size of the proton*, *Nature* **466** (2010) 213.

[4] J. Golak, G. Ziemer, H. Kamada, H. Witala and W. Gloeckle, *Extraction of electromagnetic neutron form-factors through inclusive and exclusive polarized electron scattering on polarized He-3 target*, *Phys. Rev. C* **63** (2001) 034006 [nucl-th/0008008].

[5] W. Xiong et al., *A small proton charge radius from an electron–proton scattering experiment*, *Nature* **575** (2019) 147.

[6] C. Alexandrou, S. Bacchio, M. Constantinou, J. Finkenrath, K. Hadjiyiannakou et al., *Proton and neutron electromagnetic form factors from lattice QCD*, *Phys. Rev. D* **100** (2019) 014509 [1812.10311].

[7] Extended Twisted Mass collaboration, C. Alexandrou et al., *Lattice calculation of the short and intermediate time-distance hadronic vacuum polarization contributions to the muon magnetic moment using twisted-mass fermions*, *Phys. Rev. D* **107** (2023) 074506 [2206.15084].

[8] UKQCD collaboration, C. McNeile and C. Michael, *Decay width of light quark hybrid meson from the lattice*, *Phys. Rev. D* **73** (2006) 074506 [hep-lat/0603007].

[9] A. Stathopoulos, J. Laeuchli and K. Orginos, *Hierarchical Probing for Estimating the Trace of the Matrix Inverse on Toroidal Lattices*, *SIAM J. Sci. Comput.* **35** (2013) S299 [1302.4018].

[10] G. Martinelli, C. Pittori, C. T. Sachrajda, M. Testa and A. Vladikas, *A General method for nonperturbative renormalization of lattice operators*, *Nucl. Phys. B* **445** (1995) 81 [hep-lat/9411010].

[11] C. Alexandrou, M. Constantinou, T. Korzec, H. Panagopoulos and F. Stylianou, *Renormalization constants for 2-twist operators in twisted mass QCD*, *Phys. Rev. D* **83** (2011) 014503 [1006.1920].

[12] ETM collaboration, C. Alexandrou, M. Constantinou and H. Panagopoulos, *Renormalization functions for Nf=2 and Nf=4 twisted mass fermions*, *Phys. Rev. D* **95** (2017) 034505 [1509.00213].

[13] C. Alexandrou, S. Bacchio, J. Finkenrath, C. Iona, G. Koutsou et al., *Nucleon charges and σ-terms in lattice QCD*, 2412.01535.

PoS(LATTICE2024)332

[14] C. Alexandrou et al., *Moments of nucleon generalized parton distributions from lattice QCD simulations at physical pion mass*, *Phys. Rev. D* **101** (2020) 034519 [1908.10706].

[15] W. I. Jay and E. T. Neil, *Bayesian model averaging for analysis of lattice field theory results*, *Phys. Rev. D* **103** (2021) 114502 [2008.01069].

[16] E. T. Neil and J. W. Sitison, *Improved information criteria for Bayesian model averaging in lattice field theory*, *Phys. Rev. D* **109** (2024) 014510 [2208.14983].

[17] Extended Twisted Mass collaboration, C. Alexandrou, S. Bacchio, M. Constantinou, J. Finkenrath, R. Frezzotti et al., *Nucleon axial and pseudoscalar form factors using twisted-mass fermion ensembles at the physical point*, *Phys. Rev. D* **109** (2024) 034503 [2309.05774].

[18] S. Galster, H. Klein, J. Moritz, K. H. Schmidt, D. Wegener et al., *Elastic electron-deuteron scattering and the electric neutron form factor at four-momentum transfers* $5fm^{-2} < q^2 < 14fm^{-2}$, *Nucl. Phys.* **B32** (1971) 221.

[19] Z. Ye, J. Arrington, R. J. Hill and G. Lee, *Proton and Neutron Electromagnetic Form Factors and Uncertainties*, *Phys. Lett. B* **777** (2018) 8 [1707.09063].

[20] Particle Data Group collaboration, S. Navas et al., *Review of particle physics*, *Phys. Rev. D* **110** (2024) 030001.

[21] C. Alexandrou, S. Bacchio, C. Iona, G. Koutsou, Y. Li et al., *Nucleon axial, tensor, and scalar charges and σ-terms in lattice QCD*, *PoS* **LATTICE2024** (2025) 316.

PoS(LATTICE2024)332